Journal of Computers Vol. 32 No. 6, 2021, pp. 122-133
doi:10.53106/199115992021123206010

Analysis, Design and Implementation of a Non-isolated DC-DC Converter with Low Stress

Shao-Ru Zhang[1,2], Li-Jun Wang[3], Wei Jiang[1], Xiu-Ju Du[1*], Bing Li[1], Wen-Xiu Yang[1], Yan-Hua Zhang[1], Ping-Jun Wang[1], Zhan-Ping Huang[1], Fang-Lin Luo[4]

[1] College of China Gas Technology, Hebei Normal University, No.20 East of South 2nd Ring Road, Shijiazhuang, China
shaoruzhang@mail.hebtu.edu.cn, jiangwei95@yeah.net, dxj_hbsd@126.com, linuocao@163.com, yangwx609@163.com, zyh77@sina.cn, junpw3158@126.com, hzp6617287@163.com

[2] Provincial Collaborative Innovation Center of Industrial Energy-saving and Power Quality Control, Anhui University HeFei, China

[3] Shijiazhuang Road & Bridge Facilities Management and Protection Center, Shijiazhuang, China
wanglijunfz@126.com

[4] Electrical and Electronic Engineering, Nanyang Technological University, Nanyang Avenue, Singapore
eflluo@ntu.edu.sg

Received 1 May 2021; Revised 7 June 2021; Accepted 8 June 2021

Abstract. A high gain DC/DC (HG-DC/DC) converter and a second-generation HG-DC/DC (SGHG-DC/DC) converter are proposed in this paper. The proposed converter has a new boost unit. The continuous-conduction mode (CCM) operation of the proposed converter is analyzed. Theoretical analysis shows that the proposed converters have a special U-shaped gain curve, which can achieve high gain by increasing or decreasing duty cycle. Finally, an experimental prototype with a maximum power efficiency of 91% is built to confirm the correctness of the theoretical derivation and analysis.

Keywords: High voltage gain, Boost unit, Low voltage stress

1 Introduction

Recently, renewable energy sources such as photovoltaic (PV) panels and tidal energy have drawn the attention of most scholars [1-4]. Photovoltaic grid-connected systems usually use single or several photovoltaic cell modules as the input voltage, increase the voltage through a boost network, and finally combine them into the grid through an inverter [5-6]. However, the application of renewable energy has some challenges because of their output voltage is low. Scholars have proposed many converters to boost the low voltage of the DC power supply, which can be divided into isolated converters and non-isolated converters according to their structures [7-14].

The isolated converters include full bridge, forward, flyback, high-frequency transformer, push pull and half bridge converters [15-18]. High gain can be obtained by changing the duty cycle or switching frequency, or changing the transformer's turn ratio. At the same time, the isolated converters have some drawbacks, such as complex structure, large switching loss, low efficiency, large volume and heavy weight [19-22]. On the contrary, the non-isolated converters have the advantages of small size and high efficiency. The non-isolated converters include Boost, Buck-Boost, NHS, SL, SC, Ćuk, Zeta, Luo-converters [23-28]. These converters have the effect of increasing the output voltage. However, some problems exist in actual operation, for example high voltage and current stress on the components,

* Corresponding Author

limited boost capacity, all of which limit the application of the converters. Therefore, which converter should be selected in actual application is dependent on the requirement [29-33].

A high gain DC/DC (HG-DC/DC) converter and a second-generation HG-DC/DC (SGHG-DC/DC) converter are put forward in this paper to realize high voltage gain, low voltage stress and voltage ripple. The proposed converter has different gain curves from the traditional converter. The voltage gain curves of the proposed converters are U-shaped. The purpose of boosting voltage can be realized by reducing or increasing the duty cycle of the converter. The smaller the duty cycle is, the smaller the voltage stresses on the switches are. The theoretical derivation is further verified by the experimental results on the practical prototype.

2 HG-DC/DC Converter

The topology structure of the proposed HG-DC/DC converter is shown in Fig. 1. It is composed of switches S_1 and S_2, inductors L_1 and L_2, diodes D_1-D_3, capacitors C_1-C_3, input voltage U_{in} and load R.

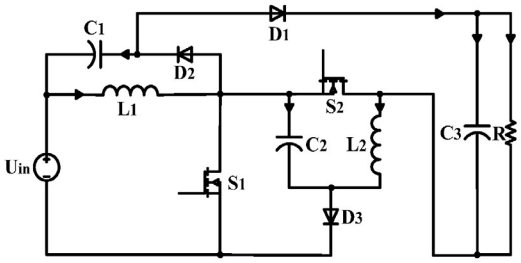

Fig. 1. The topological structure of the proposed HG-DC/DC converter

3 Boost Unit

In this section, the boost unit is proposed and extended to improve the gain of the proposed HG-DC/DC converter. Meanwhile, with the increase of the boost unit, the voltage gain rises obviously. The boost unit is shown in Fig. 2, the topologies of structural elements N = 1, 2, 3 and 4 are given.

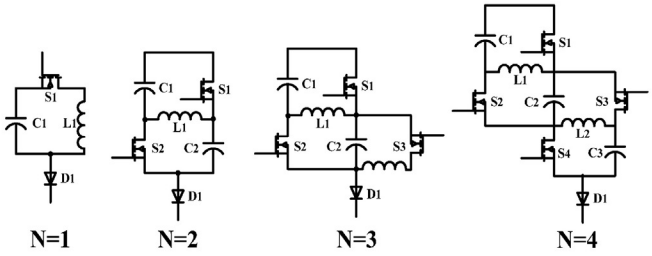

Fig. 2. Boost unit (N=1, 2, 3, 4)

4 SGHG-DC/DC Converter

To further improve voltage gain, the boost unit is added into HG-DC/DC, then the second-generation HG-DC/DC converter (SGHG-DC/DC) is formed. Take N=2 as an example, the SGHG-DC/DC converter topology is shown in Fig. 3(a).

It is composed of switches S_1-S_3, inductors L_1 and L_2, diodes D_1-D_3, capacitors C_1-C_4, power supply U_{in} and load. Among them, capacitor C_2 and C_3 form a symmetrical structure. Switches S_2, S_3 and S_1 are turned on alternately; switch duty cycle is D, and $0<D<1$. The SGHG-DC/DC converter has two operating modes, they are as follows.

Fig. 3(b) and 3(c) show the CCM operation mode, respectively.

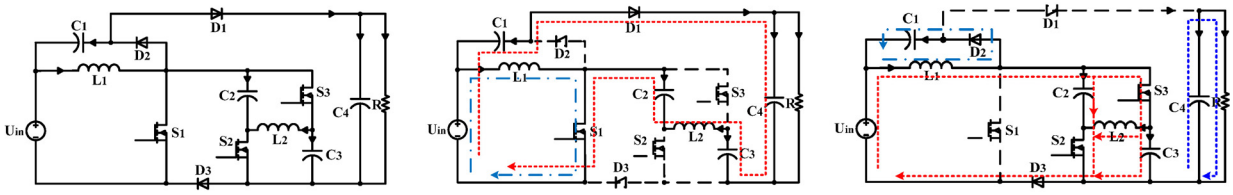

(a) the SGHG-DC/DC converter topology (b) S1 is on (c) S1 is off

Fig. 3. The topological structure of SGHG-DC/DC converter

4.1 CCM Mode Analysis of the SGHG-DC/DC Converter

When the duty cycle is 0.5, Fig. 4 shows the main waveform of SGHG-DC/DC converter; from top to bottom is: drive signal of switches S_1-S_3, the current of L_1 and L_2, the current flowing through D_1 and D_3, the voltage of C_1 and C_2.

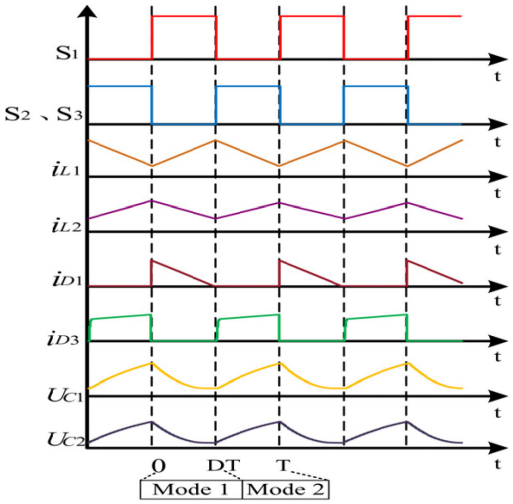

Fig. 4. The main waveform of SGHG-DC/DC converter at D=0.5

The operation of the proposed SGHG-DC/DC converter in CCM is described as follows:

In mode 1: during the period of $0 \le t \le DT$ (T is the switching cycle), switch S_1 is on; the switches S_2 and S_3 are off; and diodes D_2 and D_3 are off. And then the input voltage U_{in} charges L_1 through S_1. C_1, C_2, C_3, L_2 and U_{in} charge the load through diode D_1. Fig. 3(b) shows the equivalent circuit, and equation (1) can be obtained:

$$\begin{cases} -U_{in} + U_{L_1} = 0 \\ -U_{in} - U_{C_1} + U_R - U_{C_3} + U_{L_2} - U_{C_2} = 0 \end{cases} \quad \textbf{(1)}$$

In mode 2: during $DT < t \le T$, S_1 is turned off, S_2, S_3 and D_1 are turned on. L_1 charges C_1 through the diode D_2. U_{in} and L_1 charge C_2, C_3 and L_2 through diode D_3. C_4 charges the Load. Fig. 3(c) shows the equivalent circuit, and equation (2) can be obtained:

$$\begin{cases} U_{L_1} + U_{C_1} = 0 \\ -U_{in} + U_{L_1} + U_{C_2} = 0 \\ -U_{in} + U_{L_1} + U_{L_2} = 0 \\ -U_{C_4} + U_R = 0 \end{cases} \quad \textbf{(2)}$$

Adopted the volt-second balance of inductor, equation (3) can be gotten:

$$\begin{cases} U_{C1} = \dfrac{D}{1-D} U_{\text{in}} \\ U_{C2} = U_{C3} = \dfrac{1}{1-D} U_{\text{in}} \\ U_{C4} = \dfrac{1+2D}{D(1-D)} U_{\text{in}} \end{cases}. \tag{3}$$

Therefore, the output voltage gain G of the proposed SGHG-DC/DC converter can be gotten:

$$G = \frac{U_{\text{R}}}{U_{\text{in}}} = \frac{1+2D}{D(1-D)}. \tag{4}$$

According to equation (4), the denominator is a function with the opening downward and that the symmetrical axis is that D is equal to 0.5. Therefore, equation (4) is not a monotonic function. When D=0.37, the G of the proposed SGHG-DC/DC converter is the smallest, and a higher gain can be gotten by increasing or decreasing D.

4.2 N-Boost Unit HG-DC/DC Converter

Fig. 5 shows the topology of N-boost unit HG-DC/DC converter. It can be extended to produce a higher voltage conversion ratio by cascading boost unit.

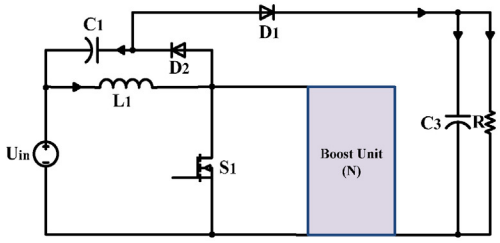

Fig. 5. N-boost unit HG-DC/DC converter

Adopting similar method for SGHG-DC/DC converter, the G of the N-boost unit HG-DC/DC converter can be obtained:

$$G = \begin{cases} \dfrac{N+1+2D}{2D(1-D)} & \text{N= odd number} \\ \dfrac{N+4D}{2D(1-D)} & \text{N=even number} \end{cases}. \tag{5}$$

4.3 Voltage gain Comparison

According to equation (4), Fig. 6(a) shows the voltage gains of the SGHG-DC/DC converter; the gain curve shows a U-shaped curve. And for comparison, the gains of the SH-SLC, SC-Boost, SL-Boost and Boost converters discussed in reference [19] are also illustrated in Fig. 6(a). The G of the SH-SLC is given by [19]:

$$G = \frac{1+3D}{1-D}. \tag{6}$$

The G of the Boost converter is:

$$G = \frac{1}{1-D}. \tag{7}$$

Compared with the gain curves of other converters, it can be seen from Fig. 6(a) that the HG-DC/DC and SGHG-DC/DC converters have higher gain when the duty cycle is same. And when the duty cycle is small, the gains of HG-DC/DC and SGHG-DC/DC converters are higher than those of the SH-SLC, SC-Boost, SL-Boost and Boost converters. It can be figured out from Fig. 6(a), at the point D = 0.37, that the minimum G of the SGHG-DC/DC converter is equal to 7.46.

Fig. 6(b) shows the G changing with the duty cycle varying when N is altered from 1 to 4. Obviously, the voltage gain of the SGHG-DC/DC converter is U-shaped curve; this type of curve has a higher voltage gain, and it can solve the problem that the duty cycle of some converters is subject to the rang 0~0.5, meanwhile, the desired output voltage can be achieved through adopting the duty cycle from 0.5 to1.

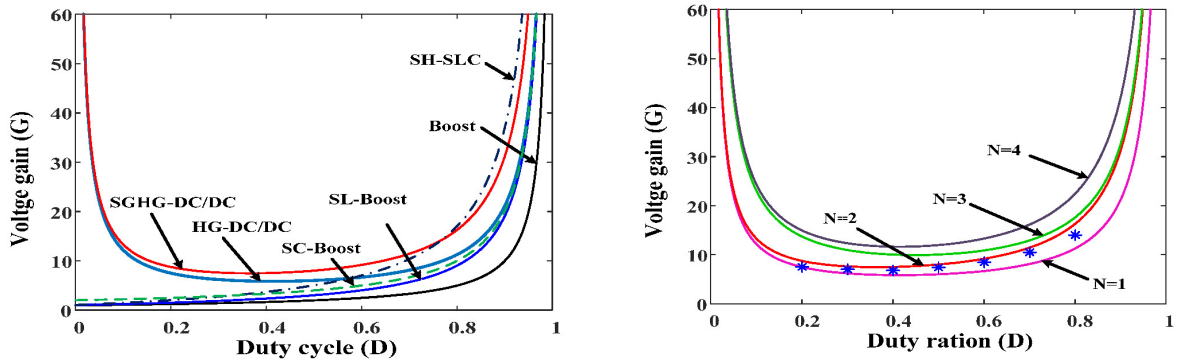

(a) voltage gains of the converters (b) voltage gains of the SGHG-DC/DC converter

Fig. 6. Voltage gain of the converters

4.4 Voltage Stress of Switches

When switch S_1 is off, the voltage stress of this switch is:

$$U_{vpS_1} = U_{C_2} = U_{L_2} = U_{C_3}. \tag{8}$$

By uniting (3), (4) and (8), equation (9) can be obtained:

$$U_{vpS_1} = \frac{1}{1-D}U_{\text{in}} = \frac{D}{1+2D}U_{\text{R}}. \tag{9}$$

When S_2, S_3 are off, the voltage stresses of the switches S_2 and S_3 are gained as equation (10):

$$\begin{cases} U_{vpS_2} = U_{L_2} + U_{C_3} \\ U_{vpS_3} = U_{L_2} + U_{C_2} \end{cases}. \tag{10}$$

By uniting (3), (4) and (10), equation (11) can be obtained.

$$\begin{cases} U_{vpS_2} = \dfrac{1}{D(1-D)}U_{\text{in}} = \dfrac{1}{1+2D}U_{\text{R}} \\ U_{vpS_3} = \dfrac{1}{D(1-D)}U_{\text{in}} = \dfrac{1}{1+2D}U_{\text{R}} \end{cases}. \tag{11}$$

Fig. 7(a) illustrates the switch voltage stresses of the HG-DC/DC and SGHG-DC/DC converters. It can be figured out from Fig. 7(a) that the voltage stresses of the proposed HG-DC/DC and SGHG-DC/DC converters are obviously lower than those of SL-Boost converter and Boost converter when the voltage gain is same. The inflection points in the diagram are the positions where the converter gain is minimal. And the switch voltage stress is obviously fewer than SC-Boost and SH-SLC converter at lower duty cycle.

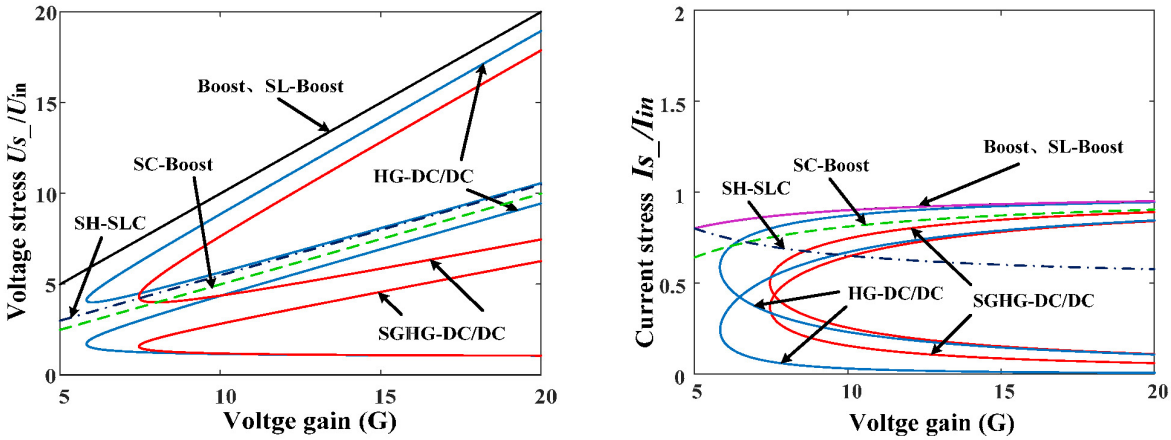

(a) the voltage stresses of switch (b) the current stresses of switch

Fig. 7. The voltage and current stresses of switch

4.5 Current Stress on Each Component

According to the principle of ampere-second balance, the average current flowing through the capacitor within one cycle is 0. According to Fig. 3, the current flowing through capacitors C_1, C_2, C_3 and C_4 is as follows:

$$\begin{cases} \int_0^{DT}(i_{L1\_on}-i_{in\_on})dt+\int_{DT}^{T}(i_{L1\_off}-i_{in\_off})dt=0 \\ \int_0^{DT}(-i_{L2\_on})dt+\int_{DT}^{T}\tfrac{1}{2}(i_{in\_off}-i_{L2\_off})dt=0 \\ \int_0^{DT}(i_{L1\_on}-i_{in\_on})dt+\int_{DT}^{T}\tfrac{1}{2}(i_{in\_off}-i_{L2\_off})dt=0 \\ \int_0^{DT}(i_{in\_on}-i_{L1\_on}-I_R)dt+\int_{DT}^{T}(-I_R)dt=0 \end{cases} . \tag{12}$$

In formula (12), i_{in_on}, i_{in_off}, i_{L_on} and i_{L_off} are the input currents and the inductor currents when switch S_1 is on and off. Generally speaking, when the inductor is large enough, the inductor under different modes meets the following requirements:

$$I_L=\frac{1}{DT}\int_0^{DT}i_{L\_on}dt=\frac{1}{(1-D)T}\int_{DT}^{T}i_{L\_off}dt\,. \tag{13}$$

Substituting equation (13) into (12), it can be obtained:

$$\begin{cases} I_{L1}=\dfrac{1+2D}{D(1-D)}I_R \\ I_{L2}=\dfrac{1}{D}I_R \end{cases} . \tag{14}$$

When the switches are turned on, the current flowing through the switches can be obtained:

$$\begin{cases} i_{S1}=\dfrac{2+D}{D(1-D)}I_R \\ i_{S2}=i_{S3}=\dfrac{1}{D(1-D)}I_R \end{cases} . \tag{15}$$

Fig. 7(b) exhibits the switch current stresses of the proposed HG-DC/DC and SGHG-DC/DC converters. It can be figured out from Fig. 7(b) that the switch current stresses of the proposed HG-DC/DC and SGHG-DC/DC converters are obviously lower than those of SL-Boost converter and Boost converter when the voltage gain is same. And the switch current stress is obviously lower than SC-Boost converter and SH-SLC converter at lower duty cycle.

4.6 Efficiency Calculation

The switches losses include switching loss and conduction loss. The switches losses can be described as equation (16):

$$P_S = P_{Sw} + P_{rs} = \sum_{i=1}^{3} P_{Sw_i} + \sum_{i=1}^{3} r_{S_i} I^2_{S_i(rms)} \,. \tag{16}$$

where P_s, P_{rs} and P_{sw} represent the total losses of the switches, switches conduction losses, and switching losses, respectively; $I_{Si(rms)}$ is the effective current passing through switches when the proposed converter switches are turned on. Switches conduction loss is expressed as equation (17):

$$\begin{cases} P_{rS_1} = r_{S_1} \cdot I^2_{S1(rms)} = \dfrac{(2+D)^2}{D(1-D)^2} \dfrac{P_o}{R} r_{S_1} \\ P_{rS_2} = r_{S_2} \cdot I^2_{S2(rms)} = \dfrac{1}{D^2(1-D)} \dfrac{P_o}{R} r_{S_2} \\ P_{rS_3} = P_{rS_2} \end{cases} . \tag{17}$$

where r_{S1}, r_{S2}, and r_{S3} are the internal resistances of the switches S_1, S_2, S_3, respectively. When $r_{S1} = r_{S2} = r_{S3} = r_S$, switches conduction loss is expressed as equation (18):

$$P_{rs} = \frac{D^3 + 4D^2 + 2D + 2}{D^2(1-D)^2} \frac{P_o}{R} r_S \,. \tag{18}$$

Switches switching loss is expressed as equation (19):

$$\begin{cases} P_{Sw1} = \dfrac{1}{2} U_{vpS1} I_{S1} (t_r + t_f) \cdot f_s = \dfrac{(2+D)(t_r + t_f) f_s U_{in}}{2D(1-D)^2} \dfrac{P_o}{U_R} \\ P_{Sw2} = \dfrac{1}{2} U_{vpS2} I_{S2} (t_r + t_f) \cdot f_s = \dfrac{(t_r + t_f) f_s U_{in}}{2D^2(1-D)^2} \dfrac{P_o}{U_R} \\ P_{Sw3} = P_{Sw2} \end{cases} . \tag{19}$$

where t_r is the turn-on-delay-time, t_f is the turn-off-delay-time. The switches switching loss is expressed as equation (20):

$$P_{Sw} = \frac{(D^2 + 2D + 1)(t_r + t_f) f_s U_{in}}{2D^2(1-D)^2} \frac{P_o}{U_R} \,. \tag{20}$$

Diodes conduction losses are expressed as equation (21):

$$P_{VF} = V_F \cdot I_{D1} + V_F \cdot I_{D2} + V_F \cdot I_{D3} = \frac{1+3D}{D} \frac{P_o}{U_R} V_F \,. \tag{21}$$

Inductors conduction losses are expressed as equation (22). Where, r_{L1} and r_{L2} are the internal resistances of the inductors L_1 and L_2, respectively.

$$\begin{cases} P_{r_{L1}} = r_{L1} \cdot I_{L1(rms)}^2 = \dfrac{(1+2D)^2}{D^2(1-D)^2}\dfrac{P_o}{R} r_{L1} \\ P_{r_{L2}} = r_{L2} \cdot I_{L2(rms)}^2 = \dfrac{1}{D^2}\dfrac{P_o}{R} r_{L2} \end{cases} . \tag{22}$$

Capacitors conduction losses are expressed as equation (23):

$$P_{rC} = \sum_{k=1}^{4} r_{Ck} \cdot I_{Ck(rms)}^2 . \tag{23}$$

where r_{Ck} and I_{Ck} are the internal resistances and effective currents of the capacitors, respectively. And effective currents can be obtained and expressed as equation (24):

$$\begin{cases} I_{C1(rms)} = I_{C2(rms)} = I_{C3(rms)} = \dfrac{1}{\sqrt{D(1-D)}} I_R \\ I_{C4(rms)} = \sqrt{\dfrac{1-D}{D}} I_R \end{cases} . \tag{24}$$

When $r_{C1}= r_{C2}= r_{C3}= r_C$, capacitors conduction losses are expressed as equation (25).

$$P_{r_C} = \sum_{k=1}^{4} r_{Ck} \cdot I_{Ck(rms)}^2 = \frac{3}{D(1-D)}\frac{P_o}{R} r_C + \frac{1-D}{D}\frac{P_o}{R} r_{C4} . \tag{25}$$

Based on equations (16)-(25), the total power losses can be expressed in equation (26):

$$P_{losses} = P_{Sw} + P_{rs} + P_{VF} + P_{r_L} + P_{r_C} . \tag{26}$$

Therefore, the efficiency of SGHG-DC/DC can be figured out and expressed in equation (27):

$$\eta = \frac{P_o}{P_{in}} = \frac{P_o}{P_o + P_{losses}} = \frac{1}{1 + P_{losses}/P_o} . \tag{27}$$

5 Experimental Results

An experimental prototype with power of 64W is built to verify the boost capability of the SGHG-DC/DC converter. Fig. 8 demonstrates the experimental prototype of the SGHG-DC/DC converter, which includes the basic SGHG-DC/DC converter circuit, switch signal device (using 555 timer to provide switching drive signal and KD501 to lift voltage). Table 1 displays the component parameters.

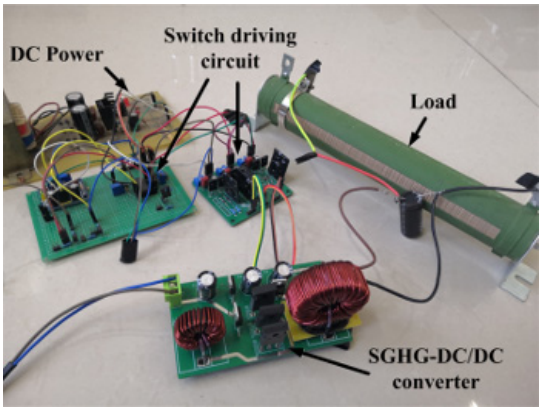

Fig. 8. The experimental prototype of SGHG-DC/DC

Table 1. The component parameters

Components	Parameters
U_{in} (input voltage range)	5V~15V
U_R (output voltage range)	35V~200V
D (duty cycle)	0.2~0.8
f_s (switching frequency)	50kHz
L_1 (inductor)	150μH, r_{L1}=20mΩ
L_2 (inductor)	1.25mH, r_{L2}=0.15Ω
C_1, C_2, C_3 (capacitors)	22μF, r_C=20mΩ
S_1, S_2, S_3 (MOSFET)	IRFB4229PBF, r_S=38mΩ
D_1, D_2, D_3 (Diodes)	MBR30100CT, V_F=0.7V
C_4 (capacitor)	470μF/450V, r_C=20mΩ
R (load)	100Ω

Taking the forward voltage drop of diodes, and the parasitic resistance of inductor and capacitor into account, the voltage gain of SGHG-DC/DC under different duty cycle conditions is shown in Table 2, which is slightly different in theory and practice. It can also be figured out from Fig. 6(b) that the theoretical value and measured value (the blue star in Fig. 6(b)) are different.

Table 2. Theoretical gain vs practical gain

D	0.2	0.3	0.4	0.5	0.6	0.7	0.8
Theoretical gain	8.75	7.62	7.5	8	9.17	11.43	16.25
Practical gain	8	7.35	7.1	7.5	8.8	10.7	14

Fig. 9 displays the experimental results of the SGHG-DC/DC with regulated input. The driving signal of every switch is illustrated in Fig. 9(a). Fig. 9(b)-(d) shows, when U_{in} =10.06V, D=0.5, the measured switch voltages, capacitor voltages and output voltage, and they are U_{S1} = U_{C2} = U_{C3} =20V, U_{S2} = U_{S3} = 40V, U_{C1} = 10V, U_R = 80V, respectively. It can be figured out from Fig. 9(e) that when the input voltage is 10.6V (purple line) and the resistance value is 10% of the rated resistance value (R_L), the output voltage is about 80V (green line). As shown in Fig. 9(f)-(h), when the input voltages are 9.2V, 11.2V and 10.8V, respectively, the output voltage is 80V, and the corresponding duty cycle is 0.6, 0.4 and 0.3. Fig. 10 shows the efficiency of SGHG-DC/DC under different load and input conditions. It can be seen that increasing the value of load and input voltage will improve the efficiency of SGHG-DC/DC.

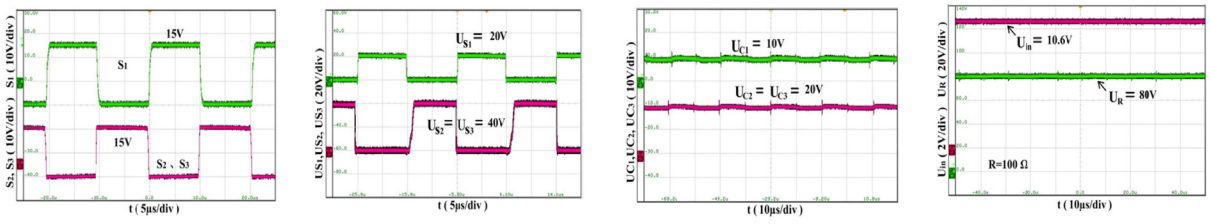

(a) the driving signal (b) the switch voltages (c) the capacitor voltages (d) D = 0.5

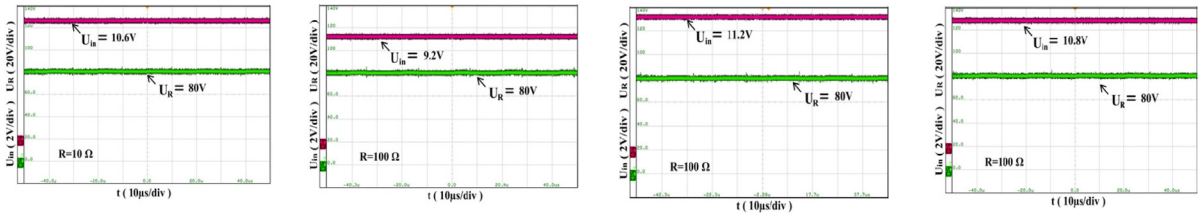

(e) D = 0.72 (f) D = 0.6 (g) D = 0.4 (h) D = 0.3

Fig. 9. The experimental waveforms of SGHG-DC/DC

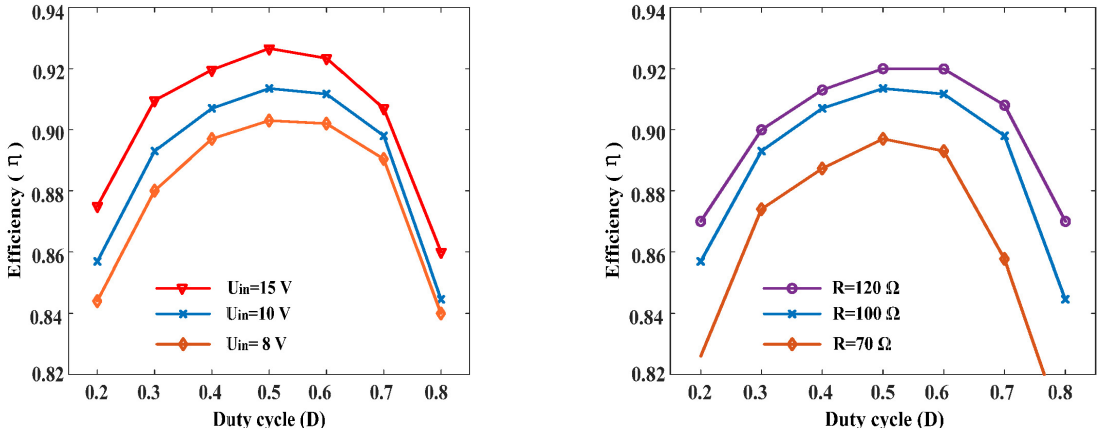

Fig. 10. Efficiency of SGHG-DC/DC at different load and input

The small signal model of the system is established, and the corresponding transfer function is obtained in equation (28):

$$\left.\frac{\tilde{u}_R}{\tilde{u}_{in}}\right|_{\tilde{d}(s)=0} = \frac{DR(2D+1)(CLs^2+1-D)}{RCDLs^2(6+4D-CLs^2)+Ls(3D^2+6D-CLs^2)+RD^2(1-D)^2}. \quad \textbf{(28)}$$

Considering the voltage gain, power efficiency, easy implementation, and system stability, the closed loop control is adopted to control the proposed converter at 0.5<D<1.

6 Conclusion

Compared with traditional converters, the proposed converter has the advantages of high gain and low stress. This paper concentrates on the detailed theoretical analysis and experimental verification for SGHG-DC/DC. It can conclude that the proposed converter overcomes the drawbacks such as low gain and high stress in traditional converters. High gain can be obtained by increasing or decreasing duty cycle, which is one of the advantages of the proposed converter.

Acknowledgements

This work was financially supported by S&T Program of Hebei (18214302D) and (19212101D), Open Project of Provincial Collaborative Innovation Center of Industrial Energy-saving and Power Quality Control, Anhui Province (KFKT201504).

In this paper, Shao-Ru Zhang and Wei Jiang contributed equally.

References

[1] E. Babaei, T. Jalizadeh, M. Sabahi, High step-up DC-DC converter with reduced voltage stress on devices, Int. Trans. Electr Energy. 29 (4)(2019) e2789.

[2] L.S. Jose, P. Vicenc, C.C. Ramon, Optimal sizing of storage elements for a vehicle based on fuel cells, supercapa citors, and batteries, Energies 12 (5)(2019) 925.

[3] M.S. Bhaskar, M. Mohammad, A. Iqbal, High gain transformer-less double-duty-triple-mode DC/DC converter for DC microgrid, IEEE Access 7 (2019) 36353-36370.

[4] R. Moradpour, H. Ardi, A. Tavakoli, Design and implementation of a new SEPIC-based high step-up DC/DC converter for renewable energy applications, IEEE Trans. Ind. Electron. 65 (2)(2017) 1290-1297.

[5] P. Padmavathi, S. Natarajan, Single switch quasi z-source based high voltage gain dc-dc converter, Int. Trans. Electr. Energy. 30 (7)(2020) e12399.

[6] Y. Zhang, H. Liu, J. Li, DC-DC boost converter with a wide input range and high voltage gain for fuel cell vehicles, IEEE Trans. Power Electron. 34 (5)(2019) 4100-4111.

[7] A. Ajami, H. Ardi, A. Farakhor, A novel high step-up DC/DC converter based on integrating coupled inductor and switched-capacitor techniques for renewable energy applications, IEEE Trans. Power Electron. 30 (8)(2015) 4255-4263.

[8] S. Danyail, S.H. Hosseini, G.B. Gharehpetian, New extendable single-stage multi-input DC-DC/AC boost converter, IEEE Trans Power Electron. 29 (2)(2014) 775-788.

[9] R.J. Wai, W.H. Wang, C.Y. Lin, High-performance stand-alone photovoltaic generation system, IEEE Trans. Ind. Electron. 55 (1)(2008) 240-250.

[10] K. Sayed, Z.M. Ali, M. Dhaifullah, Phase-shift PWM-controlled DC-DC converter with secondary-side current doubler rectifier for on-board charger application, Energies 13 (9)(2020) 2298.

[11] M. Premkumar, U. Subramaniam, H.H. Alhelou, Design and Development of Non-Isolated Modified SEPIC DC-DC Converter Topology for High-Step-Up Applications: Investigation and Hardware Implementation, Energies 13 (15)(2020) 3960.

[12] L. Yang, T. Liang, J. Chen, Transformerless DC-DC Converters With High Step-up Voltage Gain, IEEE Transactions on Industrial Electronics 56(8)(2009) 3144-3152.

[13] T. Lessa, D. Denis, J. Wesley, D. Júnior, Survey on non-isolated high-voltage step-up dc-dc topologies based on the boost converter, IET Power Electron 8(10)(2015) 2044-2057.

[14] M.A. Salvador, T.B. Lazzarin, R.F. Coelho, High step-up DC-DC converter with active switched-inductor and passive switched-capacitor networks, IEEE Transactions on Industrial Electronics 65(7)(2018) 5644-5654.

[15] H. Liu, H. Hu, H. Wu, Overview of High-Step-Up Coupled-Inductor Boost Converters, IEEE Journal of Emerging and Selected Topics in Power Electronics 4 (2)(2016) 689-704.

[16] P.K. Maroti, R. Al-Ammari, M.S. Bhaskar, New tri-switching state non-isolated high gain DC–DC boost converter for microgrid application, IET Power Electronics 12 (11)(2019) 2741-2750.

[17] D. Gu, J. Xi, L. He, A synchronous rectified flyback AC-DC converter using capacitor-coupled isolated communication, IEICE Electron. Express 17 (8)(2020) 20200013.

[18] A.A. Fardoun, E.H. Ismail, Ultra step-up DC-DC converter with reduced switch stress, IEEE Trans. Ind. Appl. 46 (5)(2010) 2025-2034.

[19] M.A. Al-Saffar, E.H. Ismail, A high voltage ratio and low stress DC-DC converter with reduced input current ripple for fuel cell source, Renew. Energy 82 (SI)(2015) 35-43.

[20] B. Bryant, M.K. Kazimierczuk, Voltage-loop power-stage transfer functions with MOSFET delay for boost PWM converter operating in CCM, IEEE Trans. Ind. Electron 54 (1)(2007) 347-353.

[21] J.C. Rosas-Caro, J.M. Ramirez, P.M. Garcia-Vite, Novel DC-DC multilevel boost converter, in: Proc. 2008 IEEE Power Electron Specialists Conference, 2008.

[22] Y. Tang, D. Fu, T. Wang, Hybrid switched-inductor converters for high step-up conversion, IEEE Trans. Ind. Electron 62 (3)(2015) 14801490.

[23] R. Amir, N. Ali, A. Hasana, An efficient branch and bound algorithm for direct model predictive control of boost converter, IEICE Electron. Express 16 (5)(2019) 20180445.

[24] S. Lee, H. Do, High step-up cascade synchronous boost DC-DC converter with zero-voltage switching, IET Power Electronics 11 (3)(2018) 618625.

[25] V. Jagan, J. Kotturu, S. Das, Enhanced-boost quasi-z-source inverters with two-switched impedance networks, IEEE Trans. Ind. Electron 64 (9)(2017) 6885-6897.

[26] X. Zhu, B. Zhang, High step-up quasi-z-source DC-DC converters with single switched capacitor branch, Journal of Modern Power Systems and Clean Energy 5 (4)(2017) 537-547.

[27] Z. Zhang, H. Zhou, C. Deng, Multiloop interleaved control for three-level buck converter in solar charging applications, IEICE Electron. Express 15 (11)(2018) 20180369.

[28] G. Wu, X. Ruan, Z. Ye, Nonisolated high step-up DC-DC converters adopting switched-capacitor cell, IEEE Trans. Ind. Electron 62 (1)(2015) 383-393.

[29] L. Liu, S. Zhang, F.L. Luo, High boost DC-DC converter: HB-LDC converter, IEICE Electron. Express 16 (6)(2019) 20181138.

[30] S.K. Kao, J.H. Wu, H.C. Cheng, All-digital controlled boost DC-DC converter with all-digital DLL-based calibration, Microelectronics journal 46 (10)(2015) 970-980.

[31] Y. Jiao, F.L. Luo, B.K. Bose, Voltage-lift split-inductor-type boost converters, IET Power Electron 4 (4)(2011) 353-362.

[32] P. Mohseni, S.H. Hosseini, M. Maalandish, Ultra-high step-up two-input DC-DC converter with lower switching losses, IET Power Electronics 12 (9)(2019) 2201-2213.

[33] P. Alavi, P. Mohseni, E. babaei, An ultra-high step-up dc-dc converter with extendable voltage gain and soft-switching capability, IEEE Trans. Ind. Electron 67 (11)(2020) 9238-9250.